Clinical Application of Autofluorescence Densitometry with a Scanning Laser Ophthalmoscope

Tetsuju Sekiryu,[1] *Tomohiro Iida,*[1] *Ichiro Maruko,*[1] *and Masayuki Horiguchi*[2]

Purpose. Fundus autofluorescence (FAF) affects the overlying absorptive retinal pigments within the eye and can potentially be used to assess their density. This study reports a clinical application of FAF in measuring photopigments by scanning laser ophthalmoscopy (SLO).

Methods. The study group comprised 20 healthy subjects, 4 patients with branch retinal artery occlusion (BRAO), 3 with macular hole, 3 with branch retinal vein occlusion (BRVO), and 4 with resolved central serous chorioretinopathy (CSC). Serial FAF images were taken during exposure to light. The intensity of the FAF was measured at the site of the macular hole or the photocoagulation laser burn in the eyes with BRVO. The autofluorescence optical density difference (fODD) was measured from the FAF images and mapped to elucidate the topographic pattern.

Results. The autofluorescence intensity showed little change at the sites of the macular holes or photocoagulation burns during exposure to light. The fODD was smallest at the center of the fovea and gradually increased with the eccentricity within 270 × 270 pixels around the fovea in healthy subjects. The amplitude of the fODD did not change in the area affected with BRAO in comparison to the unaffected area. By contrast, the fODD decreased in the area of resolved serous retinal detachment in the eyes with CSC.

Conclusions. In eyes with retinal disease, measuring the autofluorescence intensity using SLO is a feasible method of assessing the changes in the photopigments. Further studies comparing this approach with conventional methods for examining photopigments are needed. (*Invest Ophthalmol Vis Sci.* 2009;50:2994–3002) DOI:10.1167/iovs.08-2774

Fundus autofluorescence (FAF) imaging is playing increasingly important roles in diagnosing age-related macular degeneration and macular dystrophies.[1–4] FAF is generated by retinal pigment epithelium (RPE) lipofuscin,[5] which is a mixture of fluorophores that represent the digested residues of the retinal outer segments.[6] Previous studies have reported that FAF is influenced by the overlying retina.[5,7,8] The intensity of FAF may be altered by the bleaching of photopigments. Reflection densitometry is the only objective method for investigating visual photopigments in a living eye.[9–16] The possibility of applying FAF to densitometry has been suggested in a previous report.[17] The recently developed scanning laser ophthalmoscope HRA2 (Heidelberg Engineering, Heidelberg, Germany) makes it possible to observe changes in the FAF during exposure to light (Fig. 1). FAF with the HRA2 can be applied to the imaging densitometry of autofluorescence. Imaging densitometry has the advantage of assessing the topographical changes of human photopigments compared with single-spot densitometry.[13,18] Unlike in reflectometry with scanning laser ophthalmoscopy (SLO), in densitometry using FAF, the optical crosstalk caused by the surface of the retina and the choroid is thought to be relatively minor. However, the distribution of lipofuscin and macular pigments, pathologic changes of the RPE, and the thickness of the sensory retina may all contribute to the FAF intensity during exposure to light. The relationships between these factors and autofluorescence intensity must be known to determine the efficacy of autofluorescence densitometry. We studied the characteristics of autofluorescence optical density differences caused by photopigments using the HRA2 system.

Methods

Population

FAF images were obtained from 20 subjects (4 women and 16 men; mean age, 56 years; age range, 26–73) who were free of retinal diseases or significant cataract and corneal opacity. These individuals did not have any general diseases with the exception of hypertension. All the subjects were Japanese. No pseudophakic or aphakic eyes were included in this group. For each subject, two sessions on the same eye were conducted, more than 1 month apart. Images were acquired from only one eye per session. The FAF of the eyes with fundus diseases was also examined to illustrate the characteristics of autofluorescence optical density differences in various retinal lesions. These diseases included stage 4 macular hole ($n = 3$), long-standing branch retinal artery occlusion (BRAO; $n = 4$), and central serous chorioretinopathy (CSC; $n = 4$). To assess photocoagulated burns, we examined three patients with old branch retinal vein occlusion (BRVO; $n = 3$). The eligible patients with BRAO and BRVO from 6 to 24 months after onset had little retinal edema and retinal hemorrhage. In the patients with CSC 6 months or more after onset, serous retinal detachment (SRD) was completely resolved. We assessed the photoreceptor inner/outer segment junction (IS/OS) with optical coherence tomography (OCT) at the time of the examination. The IS/OS was well preserved in the eyes with BRAO. In the eyes with BRVO and CSC, the OCT IS/OS was disturbed in the fovea of the affected area of SRD. The tenets of the Declaration of Helsinki were observed. The Institutional Review Board of the University of Fukushima Medical School, Japan, granted approval for this project. Informed consent was obtained from all subjects and patients.

Retinal Imaging

The FAF images were recorded with an HRA2 confocal scanning laser ophthalmoscope. The wavelength of excitation was 488 nm (0.2 mW at the cornea). The detection filter transmitted light at wavelengths >500 nm. The size of the image field was 30°×30° (768 × 768 pixels). We took care to ensure that all the images covered the optic disc and the macula. The subjects were dark-adapted for 30 minutes. After achieving the required eye alignment and focusing in the infrared mode, serial FAF images were taken at a rate of 4.7 Hz for eyes with dilated pupils during a period of >40 seconds from the beginning of the acquisition. During image acquisition, the fundus was exposed to laser illumination. All the subjects and patients were instructed to gaze intensely at the external

From the [1]Department of Ophthalmology, Fukushima Medical University School of Medicine, Fukushima, Japan; and the [2]Department of Ophthalmology, Fujita Health University, Aichi, Japan.

Submitted for publication August 27, 2008; revised December 17, 2008; accepted April 13, 2009.

Disclosure: **T. Sekiryu**, None; **T. Iida**, None; **I. Maruko**, None; **M. Horiguchi**, None

The publication costs of this article were defrayed in part by page charge payment. This article must therefore be marked "*advertisement*" in accordance with 18 U.S.C. §1734 solely to indicate this fact.

Corresponding author: Tetsuju Sekiryu, 960-1295, 1 Hikarigaoka, Fukushima City, Fukushima Pref., Japan; sekiryu@fmu.ac.jp.

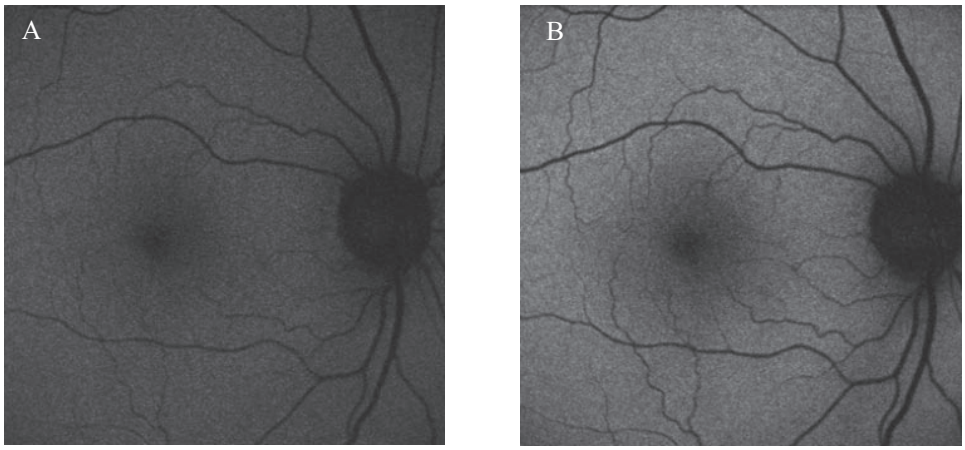

FIGURE 1. Changes of autofluorescence images caused by exposure to light. (**A**) Autofluorescence image at the beginning of observation using HRA2. (**B**) Autofluorescence image after a 40-second observation. The intensity of autofluorescence was increased by the bleaching of photopigments.

fixation light with the fellow eye (that is, the eye that was not being examined). The layer structure of the retina was examined by spectral domain (SD)-OCT using the 3D-OCT-TM system (Topcon, Tokyo, Japan) and Cirus-TM HD-OCT (Carl Zeiss Meditec, Jena, Germany).

Image Analysis

Before analysis, the serial FAF images were aligned to fix the viewpoint by using the software installed in the HRA2 system. The movie files were output as AVI files for the measurements. The FAF intensity in the macular holes and areas affected by laser coagulation therapy was measured after setting the square region of interest within these areas.

To measure the distribution of the FAF intensity, 9 × 9 grids of 30 × 30 pixels were allocated to the image of the fovea. The center of the grid was aligned at the darkest point in the fovea on the last of the serial images (Fig. 2A). The intensity of each point was measured as an eight-bit grayscale value on the frame of the AVI file (Glay-bal; Liberally Inc., Tokyo, Japan). Eye movement and blinking caused nonuniform illumination and regional variations of the autofluorescence intensity; these data were excluded from the analysis. To correct the slow intensity change during the image acquisition, the difference of the intensity of the vessels at the disc rim during the session was subtracted from the reading value of each grid.

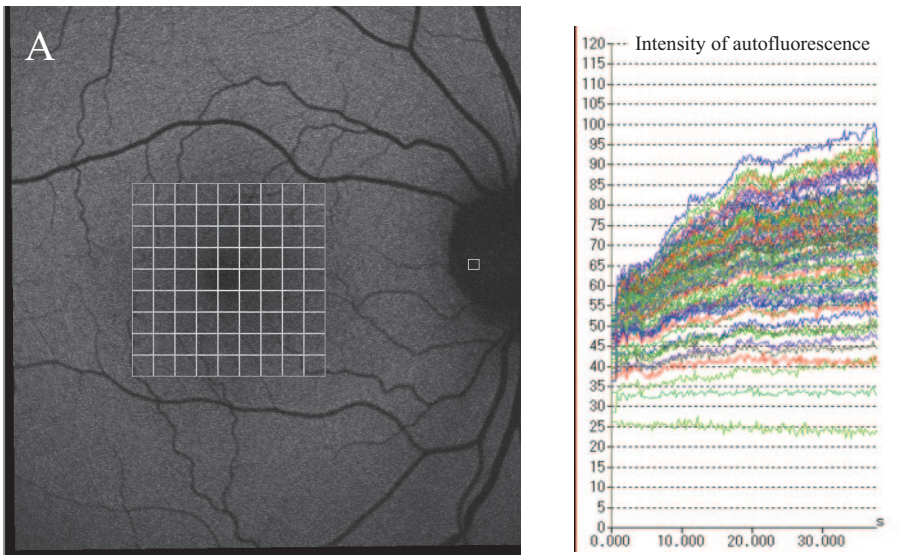

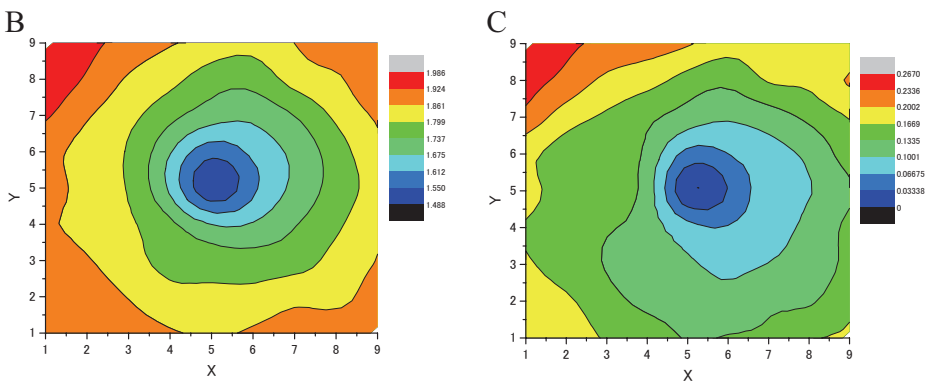

FIGURE 2. Measurement in normal subjects. (**A**) Display image of the measurement of autofluorescence intensity. The mean intensity in each cell of the 9 × 9 grid was measured and fitted to the exponential formula. (**B**, **C**) False-color maps of isointensity contours of log[*F*(end)] (**B**) and fODD (**C**). The maps were created by interpolating across each grid and assigning different colors automatically. Log[*F*(end)] was the actual value measured at the end of the measurement. fODD was calculated by fitting the logarithm of autofluorescence to equation 2.

Data Analysis

To estimate the ODD, the grayscale value during exposure to light was fitted to the following formula. During bleaching, the fraction of photopigments can change in an exponential fashion.[9,11] The intensity of FAF at time t was described as

$$F(t) = F(\infty) \times 10^{[-\mathrm{fODD} \times \exp(-kt)]} \quad (1)$$

where $F(t)$ is the measured autofluorescence at time t, $F(\infty)$ is the autofluorescence at an infinite time when the $F(t)$ approaches a constant level, fODD is the optical density difference of the pigment between the dark-adapted density and the density of the pigment after an infinitely long duration, and k is the time constant relating the chromophore properties and the intensity of light at the site of measurement. After taking the log of both sides,

$$\log[F(t)] = \log[F(\infty)] - \mathrm{fODD} \times \exp(-kt) \quad (2)$$

we fitted the logarithmic value of the FAF intensity to equation 2 on a least-squares basis with the Levenberg-Marquardt method, which gives the three unknown parameters (log[$F(\infty)$], fODD, and k), with commercial computer software (Origin 8; OriginLab Corp., Northampton, MA). In this method, log[$F(\infty)$] is calculated by extrapolation. The fODD is given as the value when the log(F) reaches a constant level. The results were displayed using a contour map classified into 11 phases. When the intensity of autofluorescence decreased or the change of the autofluorescence intensity was too small to fit equation 2 at the site of measurement, the fODD of the site was treated as 0.

To compare the distribution of FAF, the logarithmic value of the grayscale at the end of the measurement (log[F(end)]) was mapped in the same manner. The value of log[F(end)] was the actual value near log[$F(\infty)$], but was not the same as log[$F(\infty)$].

Statistical Methods

The differences of log[$F(\infty)$], fODD, and k at the temporal fourth grid in two sessions were analyzed by the paired t-test. To evaluate the symmetry of the intensity of FAF (log[F(end)] and the fODD, we compared the mean and SD at the symmetrical site of the grid on vertical and horizontal lines through the center of the fovea. The difference at the symmetrical site was tested by the paired t-test.

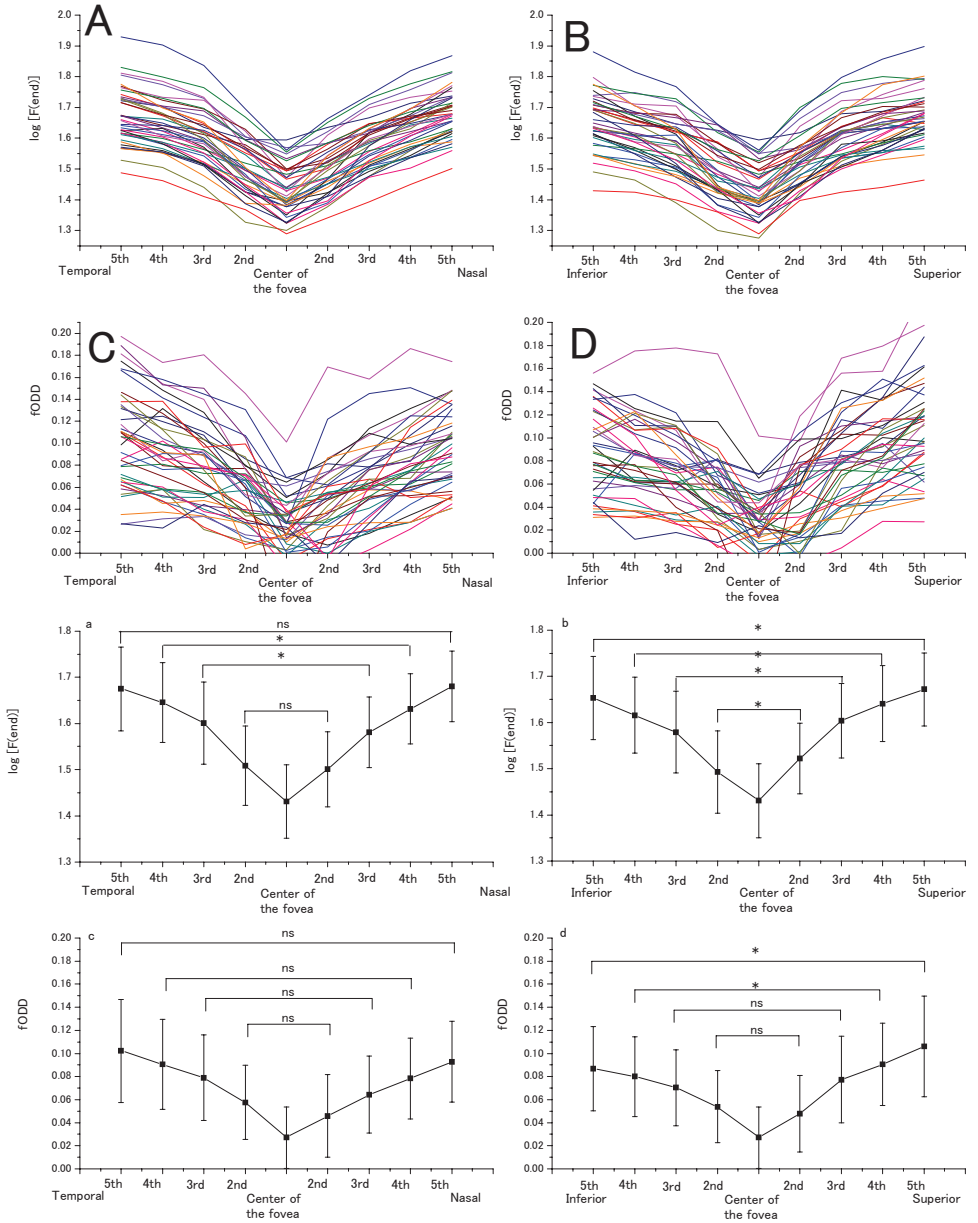

FIGURE 3. Vertical and horizontal distributions of log[F(end)] and fODD throughout the session. (**A**) Horizontal distribution of log[F(end)]. (**B**) Vertical distribution of log[F(end)]. (**C**) Horizontal distribution of fODD. (**D**) Vertical distribution of fODD. (**a–d**) The mean of (**A–D**), respectively. *Vertical lines* show the SD. At the fourth grid from the center of the fovea, the intensity of FAF was seen temporally, followed by nasally, superiorly, and inferiorly. The mean fODD was significantly higher superiorly than inferiorly. $^*P < 0.05$.

TABLE 1. Intensity of Autofluorescence in the Fourth Grid Temporal to the Fovea in a Total of 40 Sessions in 20 Normal Subjects

	1st Session			2nd Session		
Case	log($F\infty$)	fODD	k	log($F\infty$)	fODD	k
1	1.5551	0.0210	0.0580	1.5540	0.0372	0.0499
2	1.5563	0.0350	0.0585	1.5798	0.0473	0.0569
3	1.5820	0.0544	0.0617	1.5871	0.0602	0.0682
4	1.6627	0.0652	0.1613	1.6712	0.0580	0.1465
5	1.8006	0.0649	0.0669	1.7838	0.0940	0.0624
6	1.6353	0.0948	0.0763	1.6220	0.0868	0.0884
7	1.6023	0.1019	0.0791	1.6073	0.0840	0.0668
8	1.5950	0.0643	0.0621	1.5984	0.0809	0.0556
9	1.6404	0.1023	0.0608	1.6610	0.0988	0.0571
10	1.6972	0.0953	0.1656	1.6805	0.1131	0.0517
11	1.7072	0.1027	0.0684	1.7035	0.1245	0.0652
12	1.7258	0.1028	0.0668	1.7233	0.1273	0.0717
13	1.7168	0.1260	0.0675	1.7295	0.0992	0.0565
14	1.4581	0.1362	0.0561	1.5046	0.0580	0.0520
15	1.7120	0.1517	0.0696	1.6948	0.1532	0.0757
16	1.9072	0.1520	0.0675	1.8828	0.1581	0.0708
17	1.5716	0.1418	0.0755	1.6011	0.1483	0.0880
18	1.6228	0.0874	0.0522	1.6113	0.0762	0.0418
19	1.5549	0.1145	0.1051	1.5591	0.0937	0.1245
20	1.6731	0.1156	0.0612	1.6805	0.1131	0.0517
Ave	1.6488	0.0965	0.0770	1.6518	0.0956	0.0701
Std	0.100	0.037	0.032	0.088	0.035	0.026

The vertical and horizontal distribution is shown in Figure 3. Log[F(end)] is the logarithmic value of the grayscale at the end of the measurement. fODD is the optical density difference in FAF. k is the time constant. There was no significant difference between the two sessions according to the paired t-test. t = 0.464 [log($F\infty$)], 0.868 (fODD), and 0.2610 (k).

RESULTS

The autofluorescence intensity increased during exposure to laser light in the normal eyes (Fig. 1). The background of FAF at the beginning of acquisition was dark (Fig. 1A). The retinal vessels were clearly delineated at the end of acquisition, depending on the increase in the intensity of the background.

Healthy Subjects

Summaries of the vertical and horizontal distributions of the peak autofluorescence intensity (log[F(end)]) and the fODD are shown in Figure 3. The grayscale value at the site of measurement was corrected by the grayscale value of the disc in the same frame, which was considered to be almost constant during exposure to light. The intensity of autofluorescence (log[F(end)]) was lowest at the center of the fovea and increased gradually toward the periphery within a 270-pixel square. At the fourth grid from the center of the fovea, the intensity of FAF was seen temporally, followed by nasally, superiorly, and inferiorly. The difference in logarithmic intensity between the center of the fovea and the temporal fifth grid was 0.244 ± 0.063.

The fODD was generated by fitting to a simple exponential formula, equation 2. The fODD was smallest at the center of the contiguous eight grids. The mean fODDs were too small to fit the curve in 12 (30%) of the 40 sessions in the 20 normal eyes. In comparison with the symmetrical positions of the grids, the mean fODDs did not differ between the horizontal grids. The mean fODDs were significantly higher superiorly than inferiorly. The k value showed various distributions, rather than a specific distribution. In false-color maps of the isointensity contours of autofluorescence in the bleached state, the distribution of the log[F(end)] value showed a concentric pattern (Fig. 2B). The fODD increased gradually with the eccentricity within a 270-pixel square, but the pattern was not the same as the autofluorescence distribution (Fig. 2C). The fitting results of log[$F(\infty)$], k, and fODD were calculated at the point of the fourth grid temporal to the fovea in two sessions (Table 1). There was no significant difference between the two sessions according to the paired t-test; t was 0.464 (log($F\infty$)), 0.868 (fODD), and 0.2610 (k). Overall, for the 40 sessions, the mean ± SD values of log[$F(\infty)$], fODD, and k were 1.65 ± 0.093, 0.096 ± 0.035, and 0.073 ± 0.029, respectively.

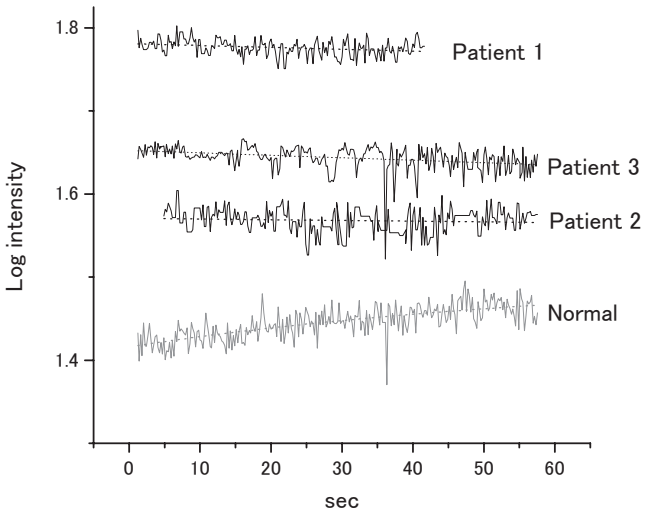

FIGURE 4. Logarithmic value of autofluorescence during exposure to light in the macular hole of three eyes from three patients. *Three black solid lines*: the logarithm of the grayscale value during exposure to light. *Dashed lines*: linear regression curves (data shown in Table 2). *Gray line*: logarithm measured at the center of the fovea in the subject shown in Figure 2, which is presented as a normal reference. The intensity of autofluorescence in the macular hole was high at the beginning of the measurement period and decreased slightly during exposure to light compared with a normal subject. The mean values of the slope of the linear regression curve for the three patients were −0.00022, −0.00009, and −0.00030, respectively.

Eyes with Diseases

Patients with macular hole showed high autofluorescence intensity compared with normal subjects at the beginning of the measurement period, which did not increase significantly during exposure to light (Fig. 4). The mean values of the slope of the linear regression curve for the three patients were −0.00022, −0.00009, and −0.00030, respectively (Table 2).

TABLE 2. Coefficient of Linear Regression Curve of Logarithm of FAF Shown in Figure 4

Patient	y Intercept	SE	Slope	SE	Fit to Eq. 2
1	1.78098	0.00144	−0.00022	5.88E-05	Failed
2	1.57071	0.0021	−0.00009	6.04E-05	Failed
3	1.65247	0.00168	−0.00030	5.01E-05	Failed
Average	1.67084	0.00339	−0.00039	1.40E-04	Failed
Normal	1.42043	0.00172	0.00085	0.00005	Success

The normal data represents the autofluorescence intensity change at the center of the fovea in the eye shown in Figure 2 and were fitted to the linear regression curve to compare the data. The fitting to the exponential formula failed in three patients with macular hole.

* Fit to Eq. 2, resultant fitting of logarithmic autofluorescence to equation 2.

The three patients with BRVO underwent laser coagulation of the affected area with a yellow laser (Multicolor Laser; Nidek, Gamagori, Japan). The fODD was decreased in the affected area with BRVO. In a 63-year-old man, the IS/OS line was distinguishable in this area, although the intensity of the intermediate line between the IS/OS line and the RPE line decreased (Figs. 5E, 5G). The FAF intensity was measured in the linearly aligned grids through the laser burn. The FAF intensity increased in the area outside of the photocoagulation burn near the vascular arcade. At the sites of the burns, the change in autofluorescence intensity during exposure to light was too slight to fit to equation 2, where SD-OCT revealed a clearly delineated IS/OS line (Figs. 5H, 5I). The change in FAF intensity after 13 of the 15 laser burns was too small to fit equation 2 (86.7%). Bleaching of the photoreceptor was not detected in most of the laser burns showing a defect of the IS/OS line.

The retina was atrophic in the affected area of eyes with long-standing BRAO at more than 3 months after onset. In a 33-year-old man, the layer structure of the inner retina disappeared on the SD-OCT images. However, the IS/OS line was well preserved. The map of the fODD demonstrated concentric patterns in the four eyes with BRAO (Fig. 6).

The fODD was measured in the four eyes with resolved CSC more than 6 months after onset. The map of the fODD was depressed in the area corresponding to the affected region of SRD, although the map of log[*F*(end)] showed hyperautofluorescence in this area. SD-OCT revealed that the IS/OS line was attenuated within the affected region (Fig. 7). The response of multifocal ERG also decreased in the inferior fovea where the fODD decreased.

The characteristics of the fODD are summarized in Table 3.

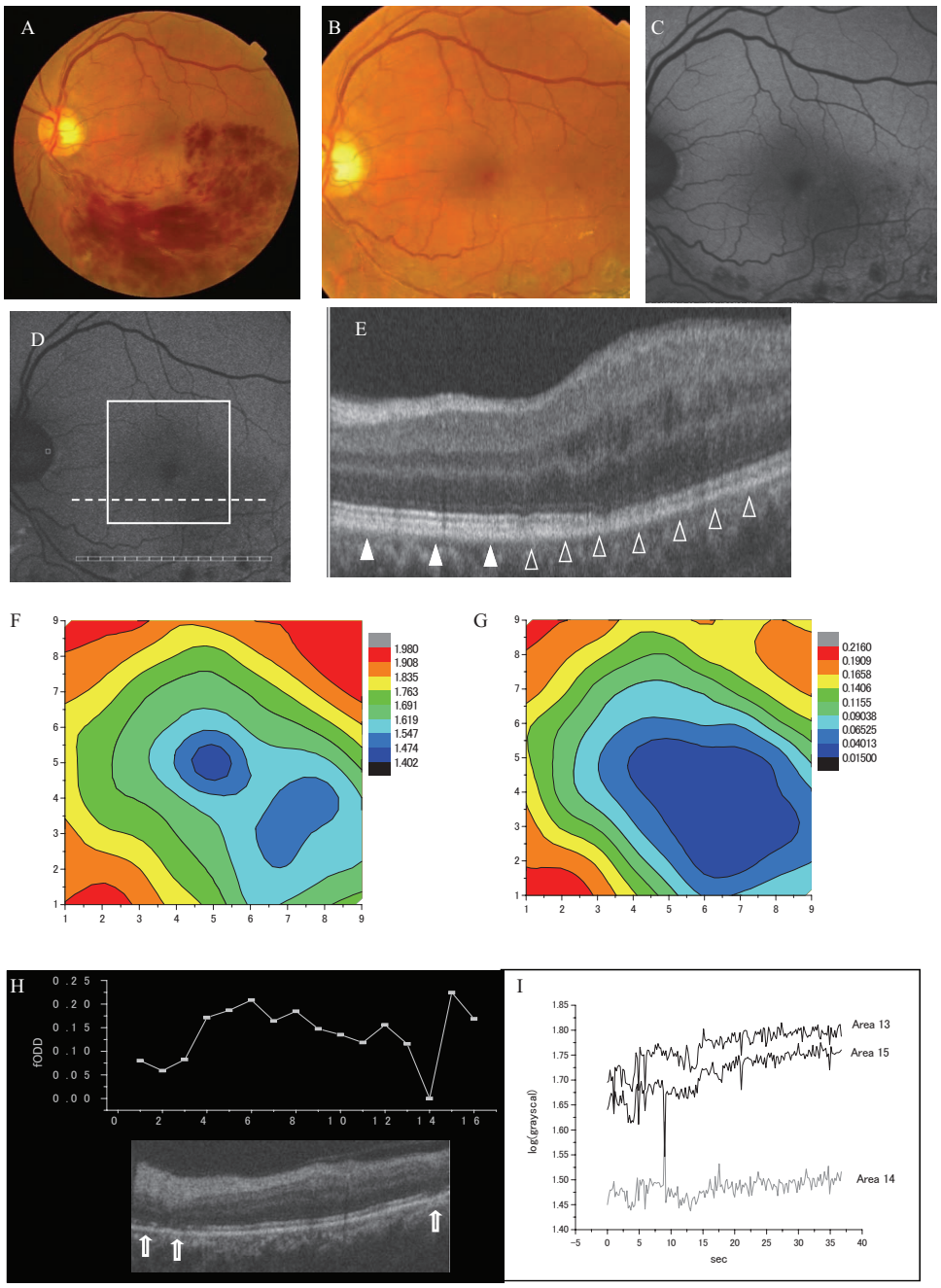

FIGURE 5. Changes of autofluorescence on laser burn in an eye with BRVO in a 63-year-old man. (**A**) Color fundus photograph at the first visit. (**B**) Color fundus photograph 10 months after onset. The hemorrhage was resolved, and laser photocoagulation burns were seen near the vascular arcade. (**C**) Image of FAF taken 10 months after onset. The intensity of autofluorescence decreased at the edge of the burns. The center of the burns showed weak autofluorescence. (**D**) The *large square* around the fovea shows the range of the measured optical density difference in (**G**). *Dashed line*: the position scanned by SD-OCT in (**E**). The 16 *small squares* near the vascular arcade indicate the positions scanned by SD-OCT and measured for fODD in (**H**) and (**I**). (**E**) SD-OCT image. The intermediate line is clearly delineated in the healthy area (*white arrowheads*). The intensity of the intermediate line decreased in the affected area (*open arrowheads*). (**F**) Color map of log[*F*(end)]. (**G**) Color map of fODD. The fODD decreased in the area affected by BRVO. (**H**) Graph showing the fODD in the 16 linearly aligned areas across the laser burn. The SD-OCT image shows the retinal tomography corresponding to the 16 areas where the fODD was measured. *White arrows*: laser burns. fODD decreased in the affected regions (areas 8–13). The laser burns (areas 2, 3, and 14) showed a further decrease of the fODD compared with the surrounding area. (**I**) The intensity of autofluorescence changed during exposure to light in areas 13 to 15. The intensity was converted to the logarithmic value. The intensity in the laser burn region (area 14) was not increased by exposure to light.

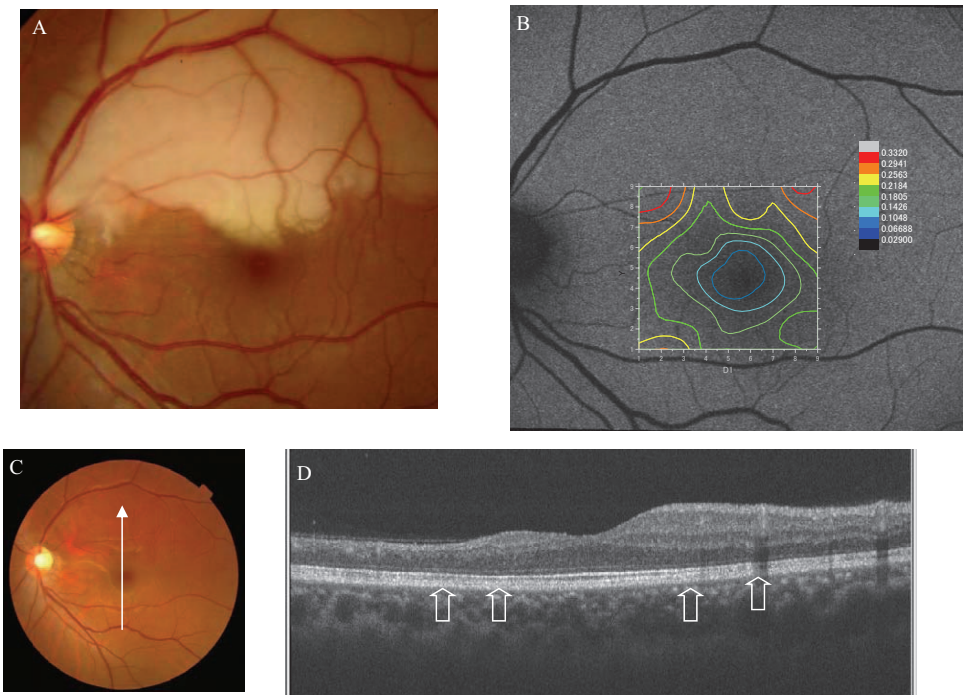

FIGURE 6. A 33-year-old patient with BRAO. (**A**) Color fundus photograph at onset. (**B**) Map of fODD overlapped with FAF image at the examination 5 months after onset. The concentric pattern of the contour map indicated that the fODD of the affected area did not decrease. (**C**) Fundus color photograph 5 months after onset. *White arrow*: the direction of the OCT scan. (**D**) The vertical OCT scan shows atrophy of the sensory retina in the affected area. The IS/OS band is not damaged even in the affected area. *Arrows*: the IS/OS line.

DISCUSSION

FAF is a useful tool for diagnosing hereditary diseases and investigating macular disorders.[3,19,20] Because autofluorescence generated by the RPE cells travels through the sensory retina, the intensity of the FAF changes according to the status of the overlying retina.[7,8] Although a change in FAF due to bleaching was reported previously,[5,17,21] this measurement has not been applied clinically. In the present study, we used autofluorescence from the RPE to evaluate photopigments, using the HRA2 (Heidelberg Engineering).

Technique

The HRA2 provides high-contrast images of FAF. However, at the beginning of the examination, it was difficult for the examinees to gaze at the same point, and the intensity of FAF was not always sufficient to be measured. Furthermore, a 40-second exposure to the HRA2 may not be sufficient for full bleaching, especially for the cone photopigments. For these reasons, we calculated the fODD, using extrapolation by fitting a simple exponential curve. This technique was used in previous reports to estimate the optical density change during bleaching.[22,23] We were able to obtain the log[$F(\infty)$], fODD, and k values from the formula. By extrapolation, we could estimate the log[$F(\infty)$] when the log(F) reached a constant level. However, a constant level of log(F) does not denote a fully bleached condition, because the photopigment can reach equilibrium through steady state illumination. The equilibrium depends on the intensity of illumination and the chromophores.[22] The intensity of the bleaching light was different at each site that was measured, because the 488-nm bleaching light was attenuated by macular pigments. When we hypothesized that the intensity of autofluorescence was constant in all areas of the fundus, the log density difference was estimated to be approximately 0.18 to 0.30, which was the difference of log[F(end)] between the fovea and the temporal fifth grid. Although this difference is mainly thought to affect the intensity of excitation light, the contribution to autofluorescence intensity cannot be estimated because the actual distribution of fluorophore density and the coefficient for autofluorescence emission are unknown. To eliminate this problem, we could use a longer wave length for excitation. For these reasons, it is difficult to determine the abnormality of the photopigment from the actual value of fODD; the map of fODD was thus created to detect the abnormality of the photopigment. When interpreting the map of fODD, one should take into consideration the influence of the macular pigment. Previous reports assessing optical density differences used the difference of the logarithmic value of the pixel.[13,24] As it is difficult to align the pictures on a pixel-to-pixel basis using this method, we measured multiple regions of interest and reconstructed a false-color map for the evaluation of the fODD.

Normal Data

The mean ± SD of 90 pixels temporal to the fovea were 0.096 ± 0.035. The fODD value was approximately 50% of that reported in previous studies using autofluorescence densitometry or reflectometry.[12,17] This difference may depend on the eccentricity of the measurement or the wavelength. The distribution patterns of FAF in the bleached condition on the vertical and horizontal lines were similar to those reported by Delori et al.[25] The fODD also showed a concentric pattern, and the fODD value in the superior retina was higher than that in the inferior retina. Because the mapping data for the fODD in 9 × 9 grids exhibited remarkable similarity to the patterns of the rod photoreceptor, it appeared mainly to represent the distribution of the optical density difference of the rods. The fODD was higher in the superior retina than in the inferior retina in the present study. A reduction of the anatomic rod density in the inferior retina with age is consistent with our results.[26] Because the excitation laser at 488 nm contributed to the results of the fODD, the absorption of the macular pigment must be considered when interpreting these data. The fODD at the center of the grids did not reach 0 in 12 sessions in six eyes. The lipofuscin excited by 488-nm light generates autofluorescence between 500 and 750 nm.[27–29] As the barrier filter of the HRA2 passes light of >500 nm, the fODD should be affected not only by rod pigments but also by cone pigments. The fODD of cones and rods is influenced mainly by the excitation light

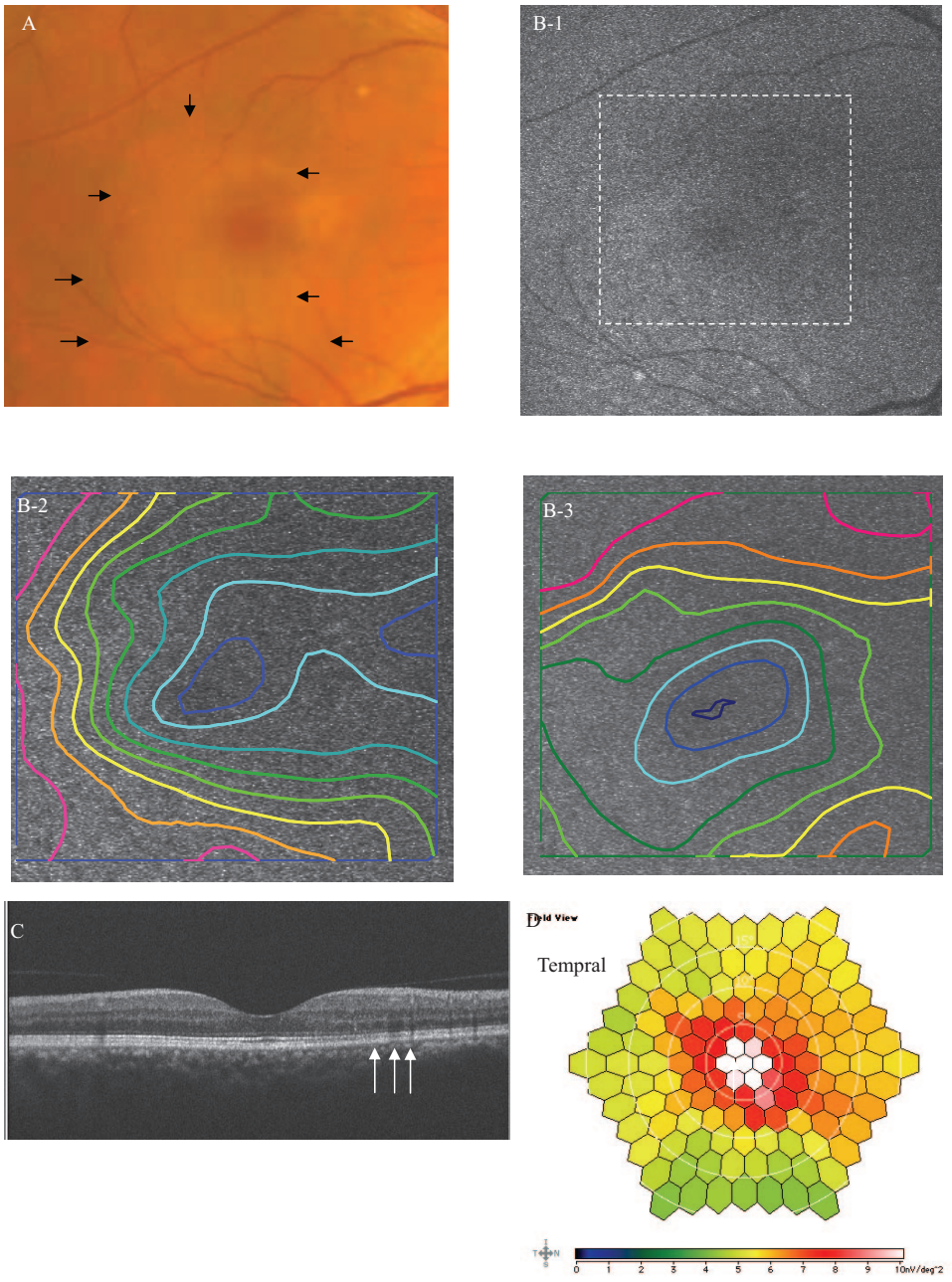

FIGURE 7. A 58-year-old man 10 months after the onset of CSC. (**A**) Color fundus photograph at the first visit showing SRD (*arrows*). (**B-1**) FAF image after resolution of SRD at the examination. *Dashed line*: the area of the measurement. (**B-2**) Overlay image of map of maximum intensity of autofluorescence (log[*F*(end)]). The intensity of autofluorescence increased from the center of the fovea to the lower temporal area. (**B-3**) Overlay image of map of fODD. The fODD decreased in the area showing hyperautofluorescence. (**C**) Vertical slice of SD-OCT image through the fovea. The intensity of the signal of the IS/OS line was attenuated in the area of hyperautofluorescence (*white arrows*). (**D**) Multifocal electroretinogram recorded at the same visit. The amplitude decreased from the temporal to inferior retina, where the response of fODD decreased.

(488 nm) rather than the emitted autofluorescence, the latter of which is not guided by the photoreceptors for cones and is absorbed less by rods.[17]

Eyes with Diseases

When the fODD is measured, the FAF intensity from the RPE should not be changed by exposure to light, even in the damaged RPE. As the RPE cells contain a substance derived from retinol,[30] the autofluorescence intensity may change during strong exposure to light. The laser power (0.2 mW) at 488 nm for the HRA2 system was higher than that reported for conventional imaging densitometry (0.07 mW).[13] We measured the autofluorescence intensity in macular holes where the RPE was directly exposed to the light, and found that the

TABLE 3. Summary of Autofluorescence Change and fODD in Various Eye Diseases

Lesions	Response of fODD	Findings of SD-OCT	
		Inner Retina	Outer Retina
Macular hole	Absent	Absent	Absent
Photocoagulation burns	Decreased	Damaged	Damaged or absent
BRAO	Normal	Damaged	Normal
CSC	Decreased	Almost normal	Damaged

intensity of FAF decreased slightly during exposure to light (the average of the slope was −0.00039), which may have been caused by photobleaching of the fluorophores. When the RPE is covered with the sensory retina, the contribution of this effect to the results may decrease. However, the fODD could be underestimated, because of the attenuation of autofluorescence of the RPE during exposure to light.

Moderately coagulated laser burns have autofluorescence.[31] The RPE shows both proliferation and hypertrophy histopathologically.[32] To examine the autofluorescence of the damaged RPE, we measured the autofluorescence intensity in the areas of the laser burns. At the center of the moderately coagulated laser burns in the eyes with long-standing BRVO, SD-OCT revealed disruption of the IS/OS line and atrophy of the inner retina. Because the fODD was small or absent in the laser burns, the autofluorescence from the pathologic RPE did not change during the measurement. The fODD could thus be assessed for a damaged RPE. This result suggests that the integrity of the IS/OS line in SD-OCT shows a good correspondence to the fODD response.

Focal or multifocal ERG shows a reduced response in the area affected by BRAO.[33] However, SD-OCT shows a well-preserved IS/OS line in the region of artery occlusion.[34] The impact on the outer segment of the retina of BRAO remains controversial. To our knowledge, the response of the outer segment to light stimuli in eyes with BRAO has not been established. The fODD map of eyes with BRAO showed a concentric pattern similar to that in the eyes of the normal subjects. This result indicated that the function of the photopigment was preserved in eyes with long-standing BRAO, although the electrophysiological function of the photoreceptor cells was impaired. The dysfunction of the Müller cells may affect the difference between the fODD and the electrophysiological response.

CSC is thought to be an acute disorder of the choroid that causes SRD and damage to the retina. The amplitude of the electrophysiological response is attenuated in areas of resolved SRD.[35,36] The sensitivity according to the microperimeter is lower within the previously affected area of SRD.[37] Disturbance of the IS/OS line in the affected area was also demonstrated recently by SD-OCT.[38] A low fODD amplitude is consistent with these results and a previous report of conventional densitometry.[39] In the present study, the fODD decreased in the area showing hyperautofluorescence and IS/OS attenuation in the eye with CSC. The area showed a decrease of the fODD amplitude that corresponded to the area of decreased amplitude in the multifocal electroretinogram (Fig. 7D). A decrease of photopigment is considered to be one reason for electrophysiological impairment in resolved CSC.[40] The fODD is an acceptable measure with which to evaluate the photopigment abnormalities caused by disorders of the outer retina.

The photopigment could be assessed using the fODD in diseases involving the inner and outer retina (Table 3). SD-OCT can delineate anatomic disorders of the retina, including those in the outer segment of photoreceptor cells.[41–44] However, the function of the outer segment cannot be assessed by OCT. As we were able to assess focal abnormalities of the outer segment by autofluorescence, it could be useful in elucidating the mechanism of retinal diseases in combination with SD-OCT.

The main weaknesses of densitometry by autofluorescence are the difficulty of quantifying the amplitude of the optical density differences of photopigments due to interindividual variations in the autofluorescence and the limitations of the measurements in cases of weak FAF. These problems may be improved by using a longer wavelength laser for emission. The fODD should be affected by the optical density differences of both cone pigments and rod pigments, because of the filter set of the HRA2 system. We could not distinguish whether changes of the cone pigments or the rod pigments contributed to the fODD. Moreover, absorption by the macular pigments may have affected the fODD. However, we believe that the fODD is useful for evaluating the photopigments clinically, because it can indicate abnormalities through a comparison of the distributions on the map. In particular, the fODD is useful for investigating the relationship between autofluorescence abnormalities and photopigments.

In conclusion, we showed that densitometry with a commercially available SLO system was suitable for assessing focal abnormalities of photopigments in eyes with retinal diseases. This method may also be useful for the assessment of macular diseases clinically.

References

1. Vaclavik V, Vujosevic S, Dandekar SS, Bunce C, Peto T, Bird AC. Autofluorescence imaging in age-related macular degeneration complicated by choroidal neovascularization: a prospective study. *Ophthalmology.* 2008;115:342–346.
2. Smith RT, Chan JK, Busuoic M, Sivagnanavel V, Bird AC, Chong NV. Autofluorescence characteristics of early, atrophic, and high-risk fellow eyes in age-related macular degeneration. *Invest Ophthalmol Vis Sci.* 2006;47:5495–5504.
3. Schmitz-Valckenberg S, Bultmann S, Dreyhaupt J, Bindewald A, Holz FG, Rohrschneider K. Fundus autofluorescence and fundus perimetry in the junctional zone of geographic atrophy in patients with age-related macular degeneration. *Invest Ophthalmol Vis Sci.* 2004;45:4470–4476.
4. Holz FG, Bindewald-Wittich A, Fleckenstein M, Dreyhaupt J, Scholl HP, Schmitz-Valckenberg S. Progression of geographic atrophy and impact of fundus autofluorescence patterns in age-related macular degeneration. *Am J Ophthalmol.* 2007;143:463–472.
5. Delori FC, Dorey CK, Staurenghi G, Arend O, Goger DG, Weiter JJ. In vivo fluorescence of the ocular fundus exhibits retinal pigment epithelium lipofuscin characteristics. *Invest Ophthalmol Vis Sci.* 1995;36:718–729.
6. Eldred GE, Katz ML. Fluorophores of the human retinal pigment epithelium: separation and spectral characterization. *Exp Eye Res.* 1988;47:71–86.
7. Framme C, Roider J. Fundus autofluorescence in macular hole surgery. *Ophthalmic Surg Lasers.* 2001;32:383–390.
8. Sayanagi K, Ikuno Y, Tano Y. Different fundus autofluorescence patterns of retinoschisis and macular hole retinal detachment in high myopia. *Am J Ophthalmol.* 2007;144:299–301.
9. Alpern M, Pugh EN Jr. The density and photosensitivity of human rhodopsin in the living retina. *J Physiol.* 1974;237:341–370.
10. Rushton WA, Campbell FW. Measurement of rhodopsin in the living human eye. *Nature.* 1954;174:1096–1097.
11. van Norren D, van der Kraats J. A continuously recording retinal densitometer. *Vision Res.* 1981;21:897–905.
12. Liem AT, Keunen JE, van Norren D, van de Kraats J. Rod densitometry in the aging human eye. *Invest Ophthalmol Vis Sci.* 1991;32:2676–2682.
13. Tornow RP, Stilling R, Zrenner E. Scanning laser densitometry and color perimetry demonstrate reduced photopigment density and sensitivity in two patients with retinal degeneration. *Vision Res.* 1999;39:3630–3641.
14. Kemp CM, Faulkner DJ. Rhodopsin measurement in human disease: fundus reflectometry using television. *Dev Ophthalmol.* 1981;2:130–134.
15. Elsner AE, Burns SA, Beausencourt E, Weiter JJ. Foveal cone photopigment distribution: small alterations associated with macular pigment distribution. *Invest Ophthalmol Vis Sci.* 1998;39:2394–2404.
16. Hood C, Rushton WA. The Florida retinal densitometer. *J Physiol.* 1971;217:213–229.
17. Prieto PM, McLellan JS, Burns SA. Investigating the light absorption in a single pass through the photoreceptor layer by means of the lipofuscin fluorescence. *Vision Res.* 2005;45:1957–1965.

18. van Norren D, van de Kraats J. Imaging retinal densitometry with a confocal scanning laser ophthalmoscope. *Vision Res.* 1989;29: 1825–1830.
19. Spaide RF. Fundus autofluorescence and age-related macular degeneration. *Ophthalmology.* 2003;110:392–399.
20. Scholl HP, Chong NH, Robson AG, Holder GE, Moore AT, Bird AC. Fundus autofluorescence in patients with Leber congenital amaurosis. *Invest Ophthalmol Vis Sci.* 2004;45:2747–2752.
21. Theelen T, Berendschot TT, Boon CJ, Hoyng CB, Klevering BJ. Analysis of visual pigment by fundus autofluorescence. *Exp Eye Res.* 2008;86:296–304.
22. Alpern M. Rhodopsin kinetics in the human eye. *J Physiol.* 1971; 217:447–471.
23. Rushton WA, Baker HD. Effect of a very bright flash on cone vision and cone pigments in man. *Nature.* 1963;200:421–423.
24. Wustemeyer H, Moessner A, Jahn C, Wolf S. Macular pigment density in healthy subjects quantified with a modified confocal scanning laser ophthalmoscope. *Graefes Arch Clin Exp Ophthalmol.* 2003;241:647–651.
25. Delori FC, Goger DG, Dorey CK. Age-related accumulation and spatial distribution of lipofuscin in RPE of normal subjects. *Invest Ophthalmol Vis Sci.* 2001;42:1855–1866.
26. Curcio CA, Sloan KR, Kalina RE, Hendrickson AE. Human photoreceptor topography. *J Comp Neurol.* 1990;292:497–523.
27. Wihlmark U, Wrigstad A, Roberg K, Brunk UT, Nilsson SE. Lipofuscin formation in cultured retinal pigment epithelial cells exposed to photoreceptor outer segment material under different oxygen concentrations. *APMIS.* 1996;104:265–271.
28. Haralampus-Grynaviski NM, Lamb LE, Clancy CM, et al. Spectroscopic and morphological studies of human retinal lipofuscin granules. *Proc Natl Acad Sci USA.* 2003;100:3179–3184.
29. Rozanowska M, Pawlak A, Rozanowski B, et al. Age-related changes in the photoreactivity of retinal lipofuscin granules: role of chloroform-insoluble components. *Invest Ophthalmol Vis Sci.* 2004;45:1052–1060.
30. Katz ML, Gao CL. Vitamin A incorporation into lipofuscin-like inclusions in the retinal pigment epithelium. *Mech Ageing Dev.* 1995;84:29–38.
31. Framme C, Brinkmann R, Birngruber R, Roider J. Autofluorescence imaging after selective RPE laser treatment in macular diseases and clinical outcome: a pilot study. *Br J Ophthalmol.* 2002;86:1099–1106.
32. Stitt AW, Gardiner TA, Archer DB. Retinal and choroidal responses to panretinal photocoagulation: an ultrastructural perspective. *Graefes Arch Clin Exp Ophthalmol.* 1995;233:699–705.
33. Kondo M, Miyake Y, Horiguchi M, Suzuki S, Tanikawa A. Clinical evaluation of multifocal electroretinogram. *Invest Ophthalmol Vis Sci.* 1995;36:2146–2150.
34. Karacorlu M, Ozdemir H, Arf Karacorlu S. Optical coherence tomography findings in branch retinal artery occlusion. *Eur J Ophthalmol.* 2006;16:352–353.
35. Moschos M, Brouzas D, Koutsandrea C, Stefanos B, Loukianou H, Papantonis F. Assessment of central serous chorioretinopathy by optical coherence tomography and multifocal electroretinography. *Ophthalmologica.* 2007;221:292–298.
36. Suzuki K, Hasegawa S, Usui T, et al. Multifocal electroretinogram in patients with central serous chorioretinopathy. *Jpn J Ophthalmol.* 2002;46:308–314.
37. Ojima Y, Tsujikawa A, Hangai M, et al. Retinal sensitivity measured with the micro perimeter 1 after resolution of central serous chorioretinopathy. *Am J Ophthalmol.* 2008;146:77–84.
38. Ojima Y, Hangai M, Sasahara M, et al. Three-dimensional imaging of the foveal photoreceptor layer in central serous chorioretinopathy using high-speed optical coherence tomography. *Ophthalmology.* 2007;114:2197–2207.
39. Chuang EL, Sharp DM, Fitzke FW, Kemp CM, Holden AL, Bird AC. Retinal dysfunction in central serous retinopathy. *Eye.* 1987;1(1): 120–125.
40. Chappelow AV, Marmor MF. Multifocal electroretinogram abnormalities persist following resolution of central serous chorioretinopathy. *Arch Ophthalmol.* 2000;118:1211–1215.
41. Koizumi H, Spaide RF, Fisher YL, Freund KB, Klancnik JM Jr, Yannuzzi LA. Three-dimensional evaluation of vitreomacular traction and epiretinal membrane using spectral-domain optical coherence tomography. *Am J Ophthalmol.* 2008;145:509–517.
42. Sakamoto A, Hangai M, Yoshimura N. Spectral-domain optical coherence tomography with multiple B-scan averaging for enhanced imaging of retinal diseases. *Ophthalmology.* 2008;115: 1071–1078.e7.
43. Srinivasan VJ, Ko TH, Wojtkowski M, et al. Noninvasive volumetric imaging and morphometry of the rodent retina with high-speed, ultrahigh-resolution optical coherence tomography. *Invest Ophthalmol Vis Sci.* 2006;47:5522–5528.
44. Wojtkowski M, Srinivasan V, Fujimoto JG, et al. Three-dimensional retinal imaging with high-speed ultrahigh-resolution optical coherence tomography. *Ophthalmology.* 2005;112:1734–1746.